Macromolecules

Article

pubs.acs.org/Macromolecules

Microstructure and Optoelectronic Properties of P3HT-*b*-P4VP/PCBM Blends: Impact of PCBM on the Copolymer Self-Assembly

Véronique Gernigon,[†,#] Patrick Lévêque,[†] Fanny Richard,[‡] Nicolas Leclerc,[‡] Cyril Brochon,[§] Christoph H. Braun,[⊥] Sabine Ludwigs,[⊥] Denis V. Anokhin,[∥,○] Dimitri A. Ivanov,[∥] Georges Hadziioannou,[§] and Thomas Heiser[†,*]

[†]Laboratoire ICube, Université de Strasbourg, CNRS UMR 7357, 23 rue du Loess, 67037 Strasbourg Cedex 2, France

[‡]Institut de Chimie et Procédés pour l'Energie, l'Environnement et la Santé (ICPEES), Université de Strasbourg, CNRS UMR 7515, 25 rue Becquerel, 67087 Strasbourg Cedex 2, France

[§]Laboratoire de Chimie des Polymères Organiques (LCPO), École Nationale Supérieure de Chimie, de Biologie et de Physique, Université Bordeaux I, 16 avenue Pey-Berland, 33607 Pessac, France

[⊥]Institut für Polymerchemie, Universität Stuttgart, Pfaffenwaldring 55, 70569 Stuttgart, Germany

[∥]Institut de Sciences des Matériaux de Mulhouse, CNRS UMR 7361, 15 rue Jean Starcky, BP 2488, Mulhouse Cedex, 68057, France

ABSTRACT: Block copolymers have been widely investigated over the past decades for their ability to microphase separate into well-defined nanostructured thin films with tailored physical properties. The aim of the present study is to investigate the thin film properties of rod−coil block copolymer/phenyl-C_{61}-butyric acid methyl ester (PCBM) blends as a function of the blend weight ratio, using a copolymer which is based on a poly(3-hexylthiophene) (P3HT) rod block and poly(4-vinylpyridine) (P4VP) coil block. Atomic force microscopy, transmission electron microscopy and grazing incidence X-ray diffraction analysis are used to study the influence of PCBM on the copolymer self-assembling. UV−visible absorption and photoluminescence spectroscopies as well as field-effect mobility measurements are performed in order to get further insight into the blend optoelectronic properties. It is found that the block copolymer phase-separated morphology and charge carrier mobilities strongly depend on the PCBM loading and thermal annealing. In particular, the results point out that PCBM enhances the block copolymer microphase separation within a narrow range of the polymer:PCBM weight ratio. In addition, clear evidence for PCBM accumulation within the P4VP domains is found by monitoring the P3HT fluorescence and charge carrier mobilities.

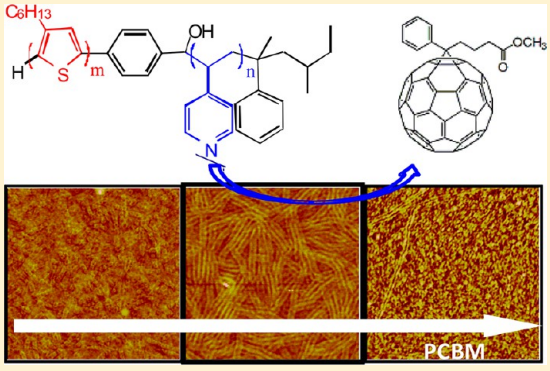

1. INTRODUCTION

Block copolymers have been widely investigated over the past decades for their ability to microphase separate into well-defined nanostructured thin films with tailored physical properties.[1−3] Rod−coil block copolymers are a special class of materials for which one block is generally a π-conjugated rigid molecular unit, while the second block is a flexible nonconjugated polymer. The conjugated segment adds an electronic functionality to the copolymer, which makes these materials of particular interest for applications in organic electronic devices.[4] The $\pi-\pi$ stacking interactions between neighboring rod blocks introduce an additional driving force that competes with Flory−Huggins phase separation and leads to a convoluted self-assembling mechanism. This gives rise to a larger variety but less understood thin film morphologies compared to those of the more standard coil−coil block copolymers.[5,6]

In recent years, rod−coil block copolymers have been investigated as active layer in organic electronic devices, such as organic thin film transistors and solar cells, or as structuring agent.[7−9] Significant efforts have been made in particular to control the synthesis of block copolymers using regioregular poly(3-hexylthiophene) (P3HT) as the conjugated block.[10] P3HT is indeed a semiconducting polymer known to self-assemble into a relatively ordered lamellar semicrystalline phase, which translates into a high hole mobility.[11,12] P3HT has also been often used as electron-donor (D) material in donor−acceptor (D−A) bulk heterojunction devices and is currently the most studied hole conducting polymer for photovoltaic applications. Recently, Yu et al. investigated P3HT-*b*-PS block copolymers with various rod/coil weight ratios and found that the block copolymer phase separation can enhance the crystallinity of the P3HT domains, leading to an increase in the hole mobility.[13] Various approaches to use P3HT based

Received: May 22, 2013
Revised: October 22, 2013
Published: November 8, 2013

block copolymers to form a nanostructured D−A heterojunction have also been reported. Botiz et al. synthesized P3HT-*b*-polylactide polymers and used them as structure-directing agent. In their case, the polylactide coil block was removed after film formation and replaced by an electron acceptor material.

Several groups reported the synthesis of P3HT based block copolymers whose coil block was functionalized with electron acceptor units (such as fullerenes).[14−17] These D−A block copolymers are expected to self-assemble spontaneously into a thermodynamically stable interpenetrated network of D and A nanodomains, approaching the ideal bulk heterojunction configuration for solar cells. The currently reported power conversion efficiencies of these devices remain however well below those achieved with state-of-the-art polymer/fullerene blends, and point out the difficulty to achieve an optimal nanomorphology.[18] For rod−coil block copolymers including a poly(butyl acrylate-*stat*-C_{60}-methylstyrene) coil block, Barrau et al. found for instance that the formation of crystalline fullerene aggregates strongly competes with the block copolymer microphase separation, leading to disordered thin films.[19] The strong tendency of covalently grafted fullerenes to form aggregates has also been observed when similar block copolymers were used as compatibilizer in P3HT/PCBM blends.[20] In the latter case, the block copolymers acted as nucleation center for PCBM crystallization.

A possible way to reduce the interference between block copolymer self-assembling and fullerene precipitation consists in using a coil block that establishes noncovalent bonds with the fullerene units. Sary et al. explored this idea by synthesizing a P3HT-*b*-P4VP block copolymer and blending it with PCBM to elaborate a D−A bulk heterojunction.[21] PCBM is indeed expected to preferentially locate within the coil phase, driven by the noncovalent bond between the Nitrogen atoms in the P4VP block and the fullerenes.[22−24] They observed that the block copolymer/fullerene blend self-assembles into nanodomains that are composed of either P3HT or P4VP rich phases. The P3HT-*b*-P4VP/PCBM layers were shown to be thermally stable and yielded promising photovoltaic performances. However, the underlying self-assembling mechanism is still poorly understood and needs to be further investigated. Very recently, Lohwasser et al. investigated the thin film morphology of pure P3HT-*b*-P4VP block copolymers with a high molecular weight P3HT block as a function of the P4VP weight fractions. Their results show in particular that microphase separation occurs even for P4VP weight fractions as high as 77%.[25]

Here, we report on the self-assembled nanostructure and optoelectronic properties of thin films composed of blends of a P3HT-*b*-P4VP block copolymer and PCBM.[26] Various block copolymer/PCBM weight ratios and annealing conditions have been explored. The nanostructure has been studied by atomic force microscopy (AFM), transmission electron microscopy (TEM) and X-ray diffraction while the opto-electronic properties have been investigated by UV−visible absorption and fluorescence spectroscopies as well as by field-effect mobility measurements. We found that PCBM has a strong impact on the copolymer self-assembling mechanism and tends to enhance the block copolymer microphase separation while hindering the crystallization process of P3HT. In particular, for a specific PCBM concentration range, a well-defined microphase separated nanostructure occurs while for pure block copolymers, processed in similar conditions, a highly disordered thin film is obtained. Moreover, evidence for PCBM accumulation within the P4VP domains is found by monitoring the P3HT fluorescence and charge carrier mobilities.

2. EXPERIMENTAL SECTION

2.1. Materials. The molecular structure of the P3HT-*b*-P4VP block copolymer used in this study is given in Scheme 1. The P3HT block has been obtained by the Grignard metathesis (GRIM) polymerization method, whereas the P4VP block has been synthesized by anionic polymerization.[27] The P4VP polymerization has been quenched by adding the aldehyde end-functionalized P3HT.[28] The molecular properties are summarized in Table 1.

Scheme 1. P3HT-*b*-P4VP Rod−Coil Block Copolymer Chemical Structure

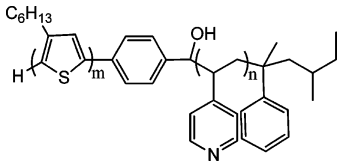

Table 1. Properties of the Copolymer

copolymer $\bar{M}_n$[a] [kg mol^{-1}]	coil block $\bar{M}_n$[a] [kg mol^{-1}]	rod block $\bar{M}_n$[a] [kg mol^{-1}]	rod block regio- regularity[a] [%]	P4VP wt fraction [%]	copolymer polydispersity
8.6	5.5	3.1	93	64	1.4

[a]Determined by ^{1}H NMR.

The coil weight fraction is approximately 64 wt %, which is significantly higher than for the copolymers used previously by Sary et al. but similar to those investigated by Lohwasser et al.[21,25] PCBM was commercially purchased and used as received. Blends of P3HT-*b*-P4VP and PCBM with various weight ratios, 1:0.32, 1:0.25, 1:0.16, and 1:0, were prepared in a 25 mg/mL chloroform solution and heated up for 24 h at 50 °C prior to spin-coating. Thin films used for morphological and optical analysis were deposited on a glass substrate covered by a 50 nm thin layer of poly(3,4-ethylenedioxythiophene):poly(styrenesulfonate) (PEDOT:PSS).

The spin-coating parameters were chosen in order to achieve a film thickness close to 200 nm, as measured by profilometry. Morphological and optoelectronic characterizations were performed on as-deposited films and after a subsequent 1 h annealing at 160 °C under nitrogen atmosphere. For some samples, an additional heat treatment at 120 °C for 24 h was applied in order to investigate the nanostructure thermal stability.

2.2. Methods. The thin film surface morphology was investigated by dynamic amplitude modulation atomic force microscopy (tapping mode) under ambient conditions. AFM observations were conducted using phase imaging on the Nanoscope IV system commercialized by Veeco. The bulk morphology was studied by transmission electron microscopy (using a 120 keV electron beam) after selective staining of the P4VP domains by exposure to iodine vapor. The thin films were removed from the substrate and collected on a TEM grid after dissolving the PEDOT:PSS layer in water.

Structural studies were performed with X-ray diffraction in grazing-incidence geometry. In these experiments, as-prepared drop-cast films, as well as films obtained upon annealing were studied. The use of drop-cast films in the X-ray diffraction experiments allowed to obtain stronger intensity of the scattering signal since the thickness of these films was higher than that of the spin-cast films used for the AFM and TEM studies. The annealing protocol included two steps: 1 h at 160 °C followed by 24 h at 120 °C. The measurements were performed on the X6B beamline at National Synchrotron Light Source (NSLS,

dx.doi.org/10.1021/ma4010692 | Macromolecules 2013, 46, 8824−8831

Brookhaven National Laboratory, Upton, NY). The X-ray energy was 10 keV. The detector used in the experiment was a Bruker Smart 1000 CCD camera. An INSTEC heating stage HCS402 equipped with a STC200 temperature controller operated under a liquid nitrogen flow was employed for variable-temperature measurements.

UV−visible absorption (using a Schimadzu UV 2101PC spectrometer) and photoluminescence (PL) measurements were done at room temperature under ambient conditions. In the case of PL spectroscopy, photoexcitation was achieved by using a pulsed laser beam at a wavelength of 355 nm. Fluctuations in film thickness, laser light intensity and photon detection efficiency were below a few percent and allow the comparison between measurements done on different samples.

For the mobility measurements, bottom gate field-effect transistors (OFET) were elaborated using available test structures commercialized by Fraunhofer IPMS. A highly doped N-type silicon sample was used as gate electrode, while a 230 nm thick thermally grown silicon oxide layer was used as gate dielectric. The lithographically patterned source and drain contacts were composed of a 30 nm thick gold layer on top of a 10 nm thick ITO adhesion layer and the channel length and width were 20 μm and 10 mm, respectively. After a cleaning step in soap, acetone and isopropyl alcohol and a 15 min exposure to ozone in an UV-ozone reactor, a thin hexamethyldisilazane (HMDS) layer was deposited by spin-coating under nitrogen atmosphere and annealed for 5 min at 130 °C. Finally, 4 mg/mL solutions of the blends were spin-coated to complete the OFET device. The samples were left overnight under vacuum to remove residual solvent traces. The device elaboration and characterizations (using an Agilent HP-4155B source measurement) were performed under nitrogen atmosphere.

3. RESULTS AND DISCUSSION

3.1. Thin Film Morphology. The AFM observations of the as-deposited pure block copolymer film and of the blends with PCBM (not shown) revealed rather featureless morphologies. Significant structural changes occurred however during the annealing step at 160 °C (1 h), as evidenced by the AFM phase images shown in Figure 1. The film morphology was found to depend strongly on the PCBM weight fraction. For the pure copolymer, the film appears like a random assembly of nanometer-sized rods (Figure 1a). No evidence for block copolymer microphase separation can be seen. On the other hand, parallel-packed well-defined lamellae are visible for both, 1:0.16 and 1:0.25 copolymer:PCBM weight ratios (Figure 1, parts b and c). The average interlamellar spacing, determined by numerical Fourier transform of the AFM phase image, increases from 22 ± 1 nm, for the lowest PCBM content, up to 27 ± 1 nm for the 1:0.25 weight ratio blend. For the highest PCBM content (1:0.32 weight ratio), the major part of the film appears again featureless with the exception of some residual double linear structures (Figure 1d). Note that similar lamellar-type structures have been observed after repeated replacements of the silicon cantilever, ascertaining that these features are not an artifact caused by a damaged tip.

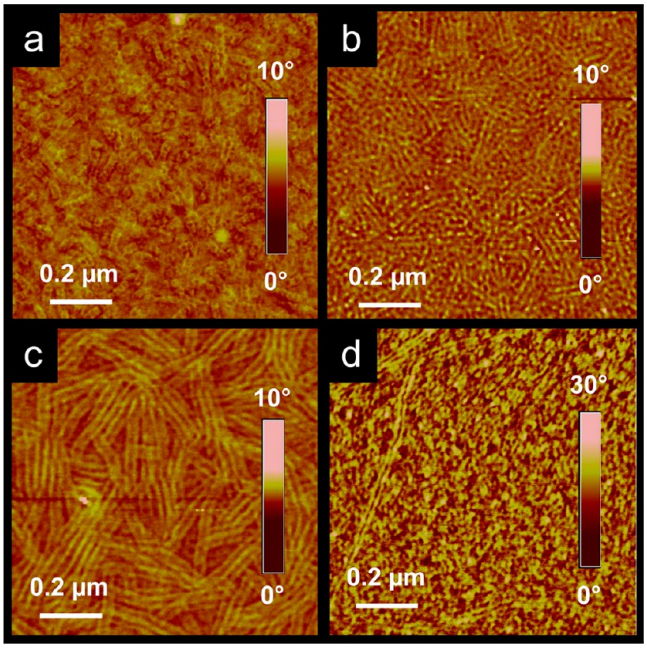

Figure 1. AFM phase images on copolymer:PCBM blends after 1 h annealing at 160 °C for different copolymer:PCBM weight ratios: (a) 1:0, (b) 1:0.16, (c) 1:0.25, and (d) 1:0.32.

Since in the AFM phase-contrast mode, lighter regions correspond generally to stiffer materials, it is likely that the bright lamellae observed in the 1:0.16 and 1:0.25 blends correspond to the rod block domains.[29,30] The higher interlamellar spacing in the 0.25 blend seem to be induced by slightly broader dark domains, as would be expected if PCBM molecules accumulate in the P4VP domains.

TEM analyses have been performed on the pure copolymer film and on the 1:0.25 blend film. Both films have been annealed at 160 °C for 1 h, followed by 24 h at 120 °C. The results are shown in Figure 2. The pure copolymer film appears as a highly disordered assembly of more or less spherical nanoaggregates, in accordance with the AFM results. No long-range order, typical for block copolymer microphase separation, can be observed for the pure copolymer, even after an extended annealing at 120 °C. This result is similar to the one observed previously by Sary et al. on a pure P3HT-*b*-P4VP block copolymer with a lower coil weight fraction and a longer P3HT block, but contrasts with the data published by Lohwasser et al. on copolymers with similar rod−coil ratios but longer rod blocks.[21,25]

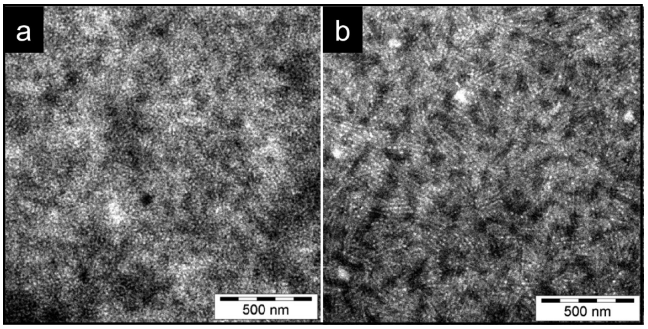

Figure 2. TEM images of the pure copolymer film (a) and of the 1:0.25 weight ratio film (b) after 1 h at 160 °C and 24 h at 120 °C.

For the 1:0.25 blend, the presence of parallel-stacked lamellae can be observed. The average interlamellar distance was estimated to 26 ± 2 nm, by taking the Fourier transform of the TEM image. This result coincides with the value determined by AFM on the 1:0.25 blend and points out that the lamellar structure observed by AFM is also present in the bulk of the film. It is also worth to note that both, AFM and TEM measurements show no presence of large PCBM crystals even after extended annealing. This behavior supports the idea that the PCBM/P4VP noncovalent bonds stabilize the blend

dx.doi.org/10.1021/ma4010692 | *Macromolecules* 2013, 46, 8824−8831

morphology by avoiding PCBM macrophase separation. The latter result substantiates the interest of P3HT-*b*-P4VP:PCBM blends for bulk heterojunction solar cell applications, for which macrophase separation of the D and A components is generally detrimental to the device lifetime.

The microstructure of pure P3HT-*b*-P4VP thin films and the corresponding blends with PCBM were investigated further by X-ray diffraction scattering in grazing-incidence geometry in wide (GIWAXS) and small (GISAXS) angles. The GIWAXS patterns corresponding to the as-cast pure copolymer film reveal the presence of P3HT crystals with the in-plane chain orientation (Figure 3a). In addition to two orders of 100 peak

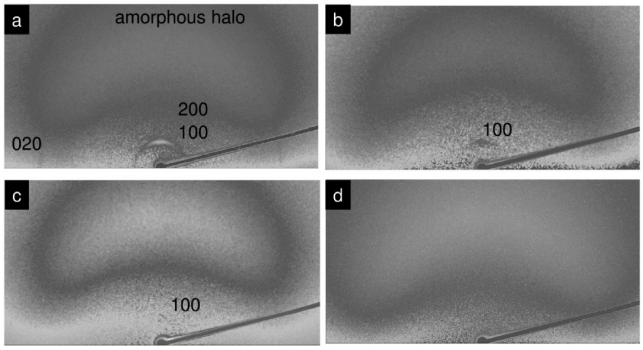

Figure 3. GIWAXS patterns corresponding to the pure copolymer before (a) and after (b) thermal annealing (1 h, 160 °C) and to the 1:0.25 copolymer:PCBM weight ratio film before (c) and after (d) thermal annealing (1 h, 160 °C).

of P3HT lattice, an intense oriented amorphous halo is visible on the meridional direction of the pattern. The 020 reflection appearing along the pattern equator reveals the formation of $\pi-\pi$ stacking parallel to the substrate. Annealing of the film leads to disappearance of higher orders of the 100 reflection and that of the 020 peak of the P3HT structure (Figure 3b). It is likely that microphase separation of the block copolymer during annealing results in deterioration of the inter- and intralayer arrangement of the P3HT block.

The blending of the copolymer with PCBM drastically changes its structure (Figure 3c). Only faint traces of the 100 peak can be found on the meridian. The increase of the amorphous halo intensity indicates a visible decrease in film crystallinity. After annealing of the film, the crystalline peaks completely disappear (Figure 3d). Hence, the presence of PCBM in the amorphous phase of the copolymer disturbs the crystal register within the P3HT domains. It is noteworthy that no peaks of the PCBM crystals were identified in the GIWAXS patterns.

The one-dimensional GISAXS curves of the nonannealed and annealed pure copolymer were found featureless (cf. curves 1 and 2 in Figure 4). However, the curves of the 1:0.25 blend reveal the form-factor of the P3HT layers (cf. curve 3 in Figure 4) corresponding to the formation of a block copolymer phase-separated morphology without crystallization of the P3HT block. The characteristic thickness of the layers calculated from the position of the form-factor minimum was estimated to be 14.1 nm. This value is in qualitative agreement with the interlamellar distances found from the analysis of TEM and AFM images. Annealing of the film was found to improve the layer-like morphology of the sample (cf. curve 4 in Figure 4).

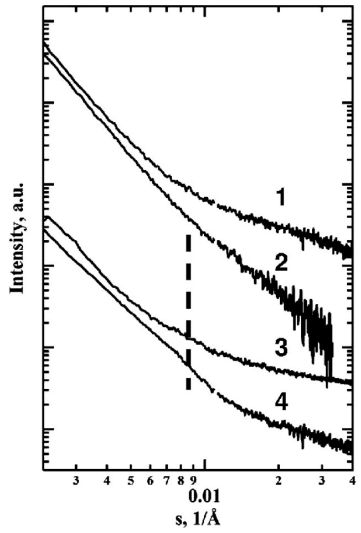

Figure 4. GISAXS curves of the pure copolymer before (1) and after (2) thermal annealing (1 h, 160 °C); the 1:0.25 copolymer:PCBM weight ratio film before (3) and after (4) thermal annealing (1 h, 160 °C). The dashed line shows the approximate position of the first minimum of the P3HT phase form-factor.

On the basis of the GISAXS, AFM, and TEM data, we may suggest that the presence of PCBM enhances the block copolymer microphase separation and induces a lamellar morphology while simultaneously hindering the crystallization process of P3HT. Rod−coil block copolymers are indeed known to microphase separate into a lamellar structure provided that the driving force toward phase-separation is large enough.[5,21] The latter is a function of the chemical incompatibility between P3HT and P4VP pair which in turn depends on the Flory−Huggins parameter χ and the degree of polymerization N. For the pure copolymer film, we did not observe the formation of lamellas even after extended annealing times, in contrast with the work reported by Lohwasser et al. on a block copolymer of similar chemical nature.[25] We attribute this discrepancy to the smaller degree of polymerization N of our copolymer, which reduces the driving force for microphase separation. As a consequence, our P3HT-*b*-P4VP copolymer may either be in the mixed phase of the equilibrium phase diagram or its microphase separation process may be kinetically quenched. Remarkably, adding relatively small amounts of PCBM while keeping the processing conditions constant, leads to a lamellar nanostructure with a well-defined homogeneous lamellar spacing, typical for microphase separated rod−coil block copolymer films.[19,30,31] We may therefore hypothesize that complexation between PCBM and P4VP enhances the chemical incompatibility between both blocks and thereby increases the driving force for microphase separation while triggering the formation of a lamellar nanostructure.

In principle, the presence of PCBM molecules may create disorder in the P3HT phase, observed by GIWAXS, according to two different mechanisms: either by increasing the driving force for microphase separation or by diffusing into the P3HT domains. The former mechanism is responsible for higher order on the mesoscopic scale, but may hinder the rod-block $\pi-\pi$ stacking interactions in the lamellar phase due to the high coil fraction of our copolymer and the related steric hindrance. The second mechanism depends on the miscibility of PCBM in the P3HT phase. By investigating the behavior of P3HT:PCBM bilayers during annealing, Treat et al. demonstrated recently

dx.doi.org/10.1021/ma4010692 | *Macromolecules* 2013, 46, 8824−8831

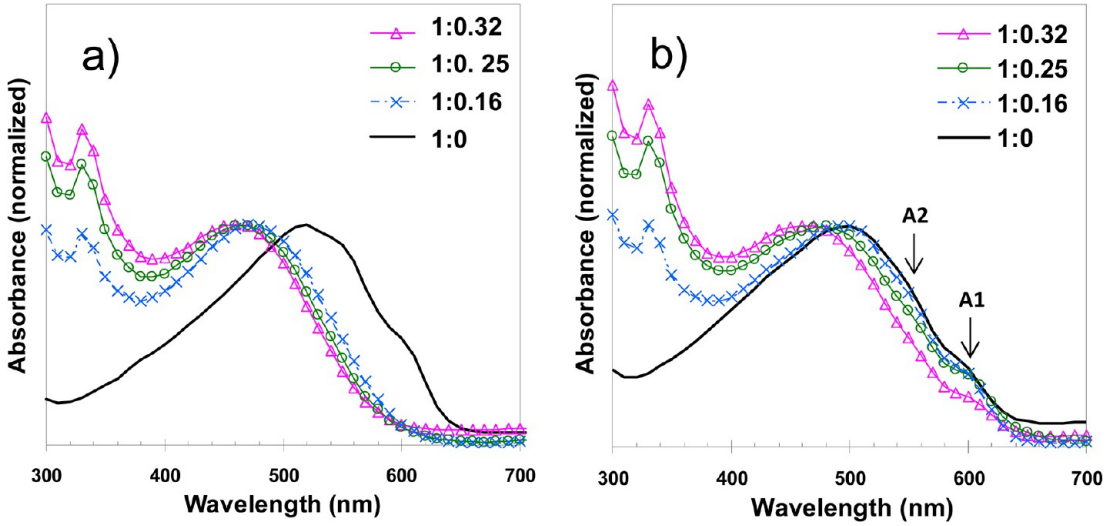

Figure 5. Normalized UV−visible spectra before thermal annealing (a) and after a (1 h, 160 °C) thermal annealing (b) as a function of copolymer:PCBM weight ratios: (red triangle and line) 1:0.32, (green circle and line) 1:0.25, (blue × and line) 1:0.16, (black line) 1:0.

that PCBM diffuses rapidly into amorphous P3HT domains even at relatively low temperature, and estimated the PCBM miscibility in P3HT to be higher than 40 wt %.[32] On the other hand, by following the optical properties of P3HT:PCBM blends, Carach et al. found that thermal annealing leads to partial crystallization of P3HT and simultaneous PCBM phase separation and aggregate formation.[33] In our case, the negligible crystallization of P3HT as revealed by GIWAXS makes the segregation mechanism described by Carach et al. unlikely. Therefore, only supramolecular interactions between PCBM and P4VP could a priori be able to promote PCBM accumulation within the P4VP domains.

In order to clarify this issue and get a better insight into the P3HT local electronic environment, it is instructive to follow the UV−visible absorption and photoluminescence spectra of P3HT-*b*-P4VP:PCBM blends, before and after thermal annealing (see next section).

In the future, it will also be interesting to analyze in more detail the interplay between ordering phenomena in the block copolymer structure and P3HT crystallization in the course of annealing, as for the compositions used in this work one can expect a significant decrease of the P3HT melting temperature.[34]

3.2. UV−Visible Absorption and Photoluminescence Spectroscopies. The normalized UV−visible absorption spectra in as-deposited thin films of the P3HT-*b*-P4VP block copolymer and of its blends with PCBM are given in Figure 5a. The spectra of annealed thin films are shown in Figure 5b. For comparison, we also included the absorption spectra of the P3HT-rod block in both, solution and solid state (Figure 6). The P3HT-rod and the as-deposited P3HT-*b*-P4VP thin films absorption spectra are almost identical, indicating that the P4VP block does not affect the conjugation length of the rod block. The P3HT-rod molecule presents a significant red-shift of their absorption edge and the appearance of vibronic peaks (arrows in Figures 5b and 6), when going from solution to solid state. The latter is attributed to the A_1 and A_2 transitions (at 600 ± 5 nm and 550 ± 10 nm, respectively), between the molecular ground state and the first and second Franck−Condon excited states, as reported by Spano for regioregular P3HT.[35] The A_1/A_2 amplitude ratio differs significantly for

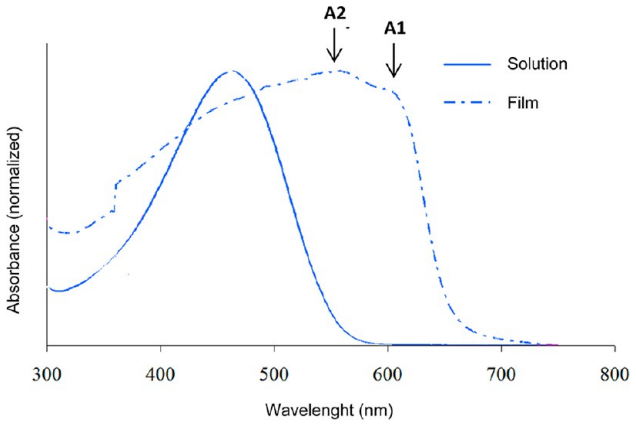

Figure 6. Normalized UV−visible spectra of P3HT-rod block in solution in dichlorobenzene and in thin film.

P3HT-rod and P3HT-*b*-P4VH materials and points out different intermolecular coupling strengths.[36] In particular, the lower amplitude ratio observed for the block copolymer (~0.5, as compared to ~0.9 for the rod block only) provides evidence for a much weaker intermolecular coupling between neighboring P3HT-rod blocks in the block copolymer film. The same absorption peaks can be observed on the annealed pure copolymer film, with reduced amplitudes but a similar amplitude ratio. This behavior can be attributed to a higher disorder (or larger amorphous fraction) of P3HT-rod and agrees with the GIWAXS results described above. The constant amplitude ratio further points out that the local molecular environment of the ordered fraction does not change considerably.

The absorption spectra of as-deposited P3HT-*b*-P4VP:PCBM blends are similar to that of the P3HT-rod molecule measured in solution, except for the peak at shorter wavelength (around 330 nm), which corresponds to PCBM exciton generation. These results indicate that the added PCBM molecules engender structural disorder and weaken the $\pi-\pi$ stacking interactions of the P3HT segments, in accordance with the X-ray diffraction data discussed above. On the annealed samples, the vibronic structure can be seen for all PCBM ratios and, for the two lowest copolymer:PCBM weight

dx.doi.org/10.1021/ma4010692 | *Macromolecules* 2013, 46, 8824−8831

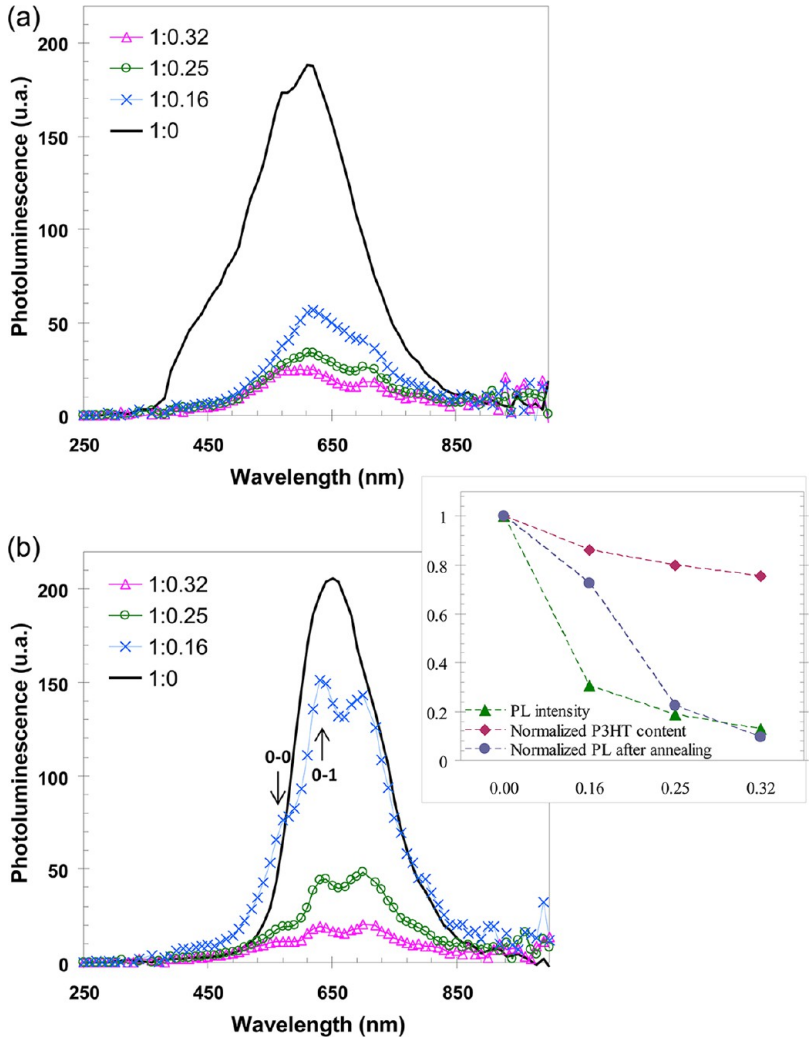

Figure 7. Photoluminescence spectra as a function of copolymer:PCBM weight ratios (a) before thermal annealing, (b) after a (1 h, 160 °C) thermal annealing. The inset corresponds to the luminescence intensity as a function of weight ratios: (red triangle and line) 1:0.32, (green circle and line) 1:0.25, (blue × and line) 1:0.16, (black line) 1:0.

ratios (1:0.16 and 1:0.25), gets close to the absorption spectrum of the pure copolymer film. Here again, the low A_1/A_2 amplitude ratio (estimated to ~0.5 ± 0.1) suggests that a rather weak intermolecular coupling between the P3HT rods occurs in the ordered P3HT domains.

The *room temperature* photoluminescence of as-deposited thin films of the P3HT-*b*-P4VP block copolymer, and of its blends with PCBM, are represented in Figure 7a. A strong decrease in luminescence intensity can be seen on the as-deposited blend films with increasing PCBM content. Since the rod block weight fraction decreases by only 20% for the 1:0.32 wt ratio with respect to the pure block copolymer film (which is significantly lower than the 70% decrease in luminescence intensity), the luminescence quenching may be attributed to the fast photoinduced charge transfer between the electron donor P3HT and the electron acceptor PCBM.

The photoluminescence spectra of annealed samples are given in Figure 7b. The figure inset shows the PL intensity as well as the P3HT fraction as a function of PCBM content. The values have been normalized by the intensity measured for the pure copolymer sample. For the 1:0.16 weight ratio, the PL intensity after annealing is significantly higher than for the as-deposited film. The PL intensity reduction observed when comparing the pure copolymer film with the 1:0.16 sample is closed to what would be expected due to the sole decrease in the P3HT weight fraction. We may therefore conclude that for this particular blend, the photoinduced charge transfer and related luminescence quenching becomes negligible. This in turn points out that significant PCBM segregation toward the P4VP phase must have occurred during annealing. Moreover, the residual PL quenching observed for the 1:0.25 sample, for which a clear microphase separation has been observed as well by AFM and TEM (see Figures 1 and 2), may be a result of either incomplete PCBM segregation toward the P4VP domains or to a more efficient charge-transfer between P3HT and PCBM molecules that are located within the P4VP phase. The latter mechanism could be an outcome of a reduced average distance between PCBM and the P3HT block with an increasing density of PCBM molecules within the P4VP lamella. The negligible increase in luminescence upon annealing seen for the 1:0.32 sample is consistent with the highly disordered morphology observed by AFM.

Interestingly, the PL spectra of the blend films display a well-defined vibronic structure, which is best resolved for the 1:0.16 weight ratio after the annealing step. The corresponding luminescence peaks are located at 573, 630, and 695 nm, and

dx.doi.org/10.1021/ma4010692 | *Macromolecules* 2013, 46, 8824−8831

are characterized by a constant energy spacing of $\Delta E = 0.18 \pm 0.01$ eV. A similar vibronic structure has been observed before on regio−regiolar P3HT polymer films by J. Clark et al. and has been described by a modified Franck−Condon progression of weakly coupled H-aggregates.[36,37] Within their model, ΔE matches the phonon energy of the C=C symmetric stretch, while the shortest wavelength peak has been attributed to a disorder allowed 0−0 transition between the zero phonon excited state and the Franck−Condon ground state of the H-aggregates. Surprisingly, the 0−0 transition energy (2.14 eV) observed for the P3HT-*b*-P4VP:PCBM blends is about 0.25 eV higher than the value reported by J. Clark et al. As a consequence, our absorption and luminescence data point out a negligible Franck−Condon shift (energy difference between the 0−0 absorption and 0−0 emission). The origin of this particular behavior remains unclear and requires a more thorough investigation of the block copolymer blend properties (for instance by measuring photoluminescence at low temperature), which lies however beyond the scope of the present report.

Nevertheless, within the framework of the H-aggregate model, we may get some more insight into the local molecular environment of the P3HT-rods, by taking into account the amplitude ratio of 0−0 and 0−1 vibronic transitions (located at 573 and 630 nm respectively) .[33,36] Indeed, the 0−0 transition is known to be forbidden in perfectly aligned H-aggregates and can only be observed in the presence of structural disorder. Therefore, high 0−0/0−1amplitude ratios are representative of high disorder in the local molecular environment. Reported values lie within 0.3 to 0.8 range.[33] For the 1:0.26 blend, the amplitude ratio is estimated to 0.9. If we assume that the coupling between the electronic transition and phonon mode for the P3HT-rod block copolymer is similar to the value reported for P3HT polymer,[36] such a high amplitude ratio indicates a disorder close to that of an isolated macromolecule in solution.[33] It is somewhat surprising, that this high disorder does not hinder the observation of the vibronic features by *room temperature* PL. Note that the vibronic structure is barely visible in the pure block copolymer film. We suggest that the confinement of the P3HT rod−block within the rod domains of the microphase-separated thin film could be responsible for this remarkable behavior.

The absorption and luminescence data are in line with the morphology results and corroborate the conclusion that the P3HT blocks within the lamellar domains of annealed copolymer:PCBM films are in a highly disordered state. As a consequence, it is unlikely that P3HT crystallization contributes to the PCBM phase segregation, as it does in standard P3HT:PCBM blends. Rather, the supramolecular interaction between PCBM and the P4VP blocks can be considered as the major driving force for the preferential accumulation of PCBM within the P4VP domains.

3.3. Field-Effect Mobility Measurements. An additional way to probe the ordering of both, the P3HT block and the PCBM molecules, consists in measuring the charge carrier mobilities. The hole mobility (μ_h) is indeed strongly dependent on the P3HT $\pi-\pi$ stacking interactions while the electron mobility (μ_e) depends on the percolation between PCBM molecules. We therefore implemented the copolymer/PCBM thin films as semiconductor layer into an organic field effect transistor and estimated the charge carrier mobilities by fitting the device transfer characteristics to a standard device model.[38] The hole mobility has been measured in the linear regime while the electron mobility has been extracted in the saturation regime. This procedure relates to the fact that the high contact resistance (R_c) for electron injection does not allow the observation of a linear regime (see below).

No field-effect could be observed in as-deposited thin films, corroborating the lack of structural order observed by AFM and optical spectroscopy. After 1 h annealing at 160 °C, the current remains below the detection limit for the transistor based on the pure block copolymer film. On the other hand, however, the devices made of the polymer/PCBM blends show an ambipolar charge transport, although with relatively low currents (see Figure 8). The small but non-negligible drain current at zero drain voltage is due to gate leakage. The extracted electron and hole mobilities as a function of PCBM content are summarized in Table 2. The values are orders of magnitude lower than those typically observed for P3HT and PCBM and make these films inappropriate for device applications. Nevertheless, the dependency of the mobilities on the PCBM content nicely fits with the conclusions outlined above. In particular, the fact that adding PCBM is necessary for the observation of a hole transport is consistent with the idea that fullerenes trigger the copolymer microphase separation giving rise to percolation paths for both, electrons and holes.

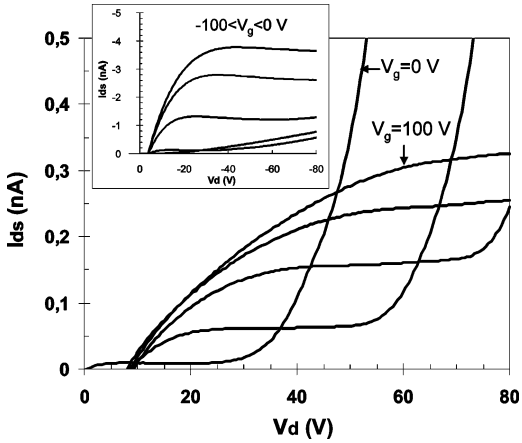

Figure 8. Ambipolar transistor transfer characteristics for a channel with 1:0.25 copolymer:PCBM weight ratio after 1 h annealing at 160 °C. The p-type transistor characteristics are illustrated in the inset.

Table 2. Electron and Hole Mobilities as a Function of Copolymer:PCBM Weight Ratio after 1 h at 160 °C

copolymer:PCBM weight	1:0	1:0.16	1:0.25	1:0.32
μ_h [cm^2/(V s)]	_	8×10^{-7}	2×10^{-6}	6×10^{-7}
μ_e [cm^2/(V s)]	_	2×10^{-8}	2×10^{-8}	3×10^{-8}

4. CONCLUSION

In conclusion, a combination of AFM, GIWAXS, and GISAXS and the optoelectronic results obtained on P3HT-*b*-P4VP/PCBM block copolymer fullerene blends give strong evidence that the presence of PCBM influences the block copolymer self-assembling. Within a specific range of PCBM concentrations, a more pronounced block copolymer microphase separation and more intense $\pi-\pi$ stacking interactions of the rod block have been observed, giving rise to ambipolar charge transport. Moreover, the luminescence increase after annealing clearly

dx.doi.org/10.1021/ma4010692 | *Macromolecules* 2013, 46, 8824−8831

shows that PCBM molecules are preferentially localized within the P4VP domains, corroborating the impact of the noncovalent interaction between the fullerene and 4VP units. Finally, the thermal stability of the blend morphology as well as the absence of PCBM crystallization confirms the ability of such blends to avoid macrophase separation which is one of the problems in state-of-the-art solar cell applications.

AUTHOR INFORMATION

Corresponding Author

*E-mail (T. H.): thomas.heiser@unistra.fr.

Present Addresses

[#]Present address (V.G.): Département Electronique Optronique et Signal (DEOS), Institut Supérieur de l'Aéronautique et de l'Espace (ISAE), 10 avenue Édouard Belin, 31055 Toulouse, France

[○]Present address (D.V.A.): Moscow State University, Faculty of Fundamental Physical and Chemical Engineering, Moscow, 119991, Russia

Notes

The authors declare no competing financial interest.

ACKNOWLEDGMENTS

The authors would like to thank the Region Alsace and the French research agency (ANR) for financial support via HABISOL program: "Spirwind". C.H.B. and S.L. thank the Emmy Noether program of the DFG for financial support. Dr. R. Thomann is acknowledged for TEM microscopy. D.V.A. and D.A.I. acknowledge the Russian Ministry of Science and Education (Grants No 11G34.31.0055 and 14.518.11.7013) for financial support.

REFERENCES

(1) Bates, F. S. *Science* **1991**, *251*, 898−905.
(2) Leibler, L. *Macromolecules* **1980**, *13*, 1602−1617.
(3) Olsen, B.; Segalman, R. A. *Mater. Sci. Eng.: R. Rep.* **2008**, *62*, 37−66.
(4) Segalman, R. A.; McCulloch, B.; Kirmayer, S.; Urban, J. J. *Macromolecules* **2009**, *42*, 9205−9216.
(5) Reenders, M.; Ten Brinke, G. *Macromolecules* **2002**, *35*, 3266−3280.
(6) Bates, F. S.; Fredrickson, G. H. *Phys. Today* **1999**, 32−38.
(7) Chueh, C. C.; Higashihara, T.; Tsai, J. H.; Ueba, M.; Chen, W. C. *Org. Electron.* **2009**, *10*, 1541−1548.
(8) Yang, C.; Lee, J. K.; Heeger, A. J.; Wudl, F. *J. Mater. Chem.* **2009**, *19*, 5416−5423.
(9) Botiz, I.; Darling, S. B. *Macromolecules* **2009**, *42*, 8211−8217.
(10) Iovu, M. C.; Jeffries El, M.; Sheina, E. E.; Cooper, J. R.; McCullough, R. D. *Polymer* **2005**, *46*, 8582−8586.
(11) Brinkmann, M.; Wittmann, J. C. *Adv. Mater.* **2006**, *18*, 860−863.
(12) Crossland, E. J. W.; Tremel, K.; Fischer, F.; Rahimi, K.; Reiter, G.; Steiner, U.; Ludwigs, S. *Adv. Mater.* **2012**, *24*, 839−844.
(13) Yu, X. K. X.; Chen, J.; Lavrik, N. K.; Hong, K.; Sumpter, B. G.; Geohegan, D. B. *ACS Nano* **2011**, *5*, 3559−3567.
(14) Sommer, M.; Huettner, S.; Thelakkat, M. *J. Mater. Chem.* **2010**, *20*, 10788−10797.
(15) Lee, J. U.; Cirpan, A.; Emrick, T.; Russell, P.; Jo, W. H. *J. Mater. Chem.* **2009**, *192*, 1483−1489.
(16) Tao, Y.; McColloch, B.; Kim, S.; Segalman, R. A. *Soft Matter* **2009**, *5*, 4219−4230.
(17) Richard, F.; Brochon, C.; Leclerc, N.; Eckhardt, D.; Heiser, T.; Hadziioannou, G. *Macromolecular Rapid Communication* **2008**, *29*, 885−891.
(18) Huettner, S.; Hodgkiss, J. M.; Sommer, M.; Friend, R. H.; Steiner, U.; Thelakkat, M. *J. Phys. Chem. B* **2012**, *116*, 10070−10078.
(19) Barrau, S.; Heiser, T.; Richard, F.; Brochon, C.; Ngov, C.; Van De Wetering, K.; Hadziioannou, G. *Macromolecules* **2008**, *41*, 2701−2710.
(20) Gernigon, V.; Lévêque, P.; Brochon, C.; Audinot, J. N.; Leclerc, N.; Bechara, R.; Richard, F.; Heiser, T.; Hadziioannou, G. *Eur. Phys. J. Appl. Phys.* **2011**, *56*, 34107.
(21) Sary, N.; Richard, F.; Brochon, C.; Leclerc, N.; Lévêque, P.; Audinot, J. N.; Berson, S.; Heiser, T.; Hadziioannou, G.; Mezzenga, R. *Adv. Mater.* **2010**, *22*, 763−768.
(22) Fujita, N.; Yamashita, T.; Asai, M.; Shinkai, S. *Angew. Chem.* **2005**, *44*, 1257−1261.
(23) Laiho, A.; Ras, R. H. A.; Valkama, S.; Ruokolainen, J.; Österbacka, R.; Ikkala, O. *Macromolecules* **2006**, *39*, 7648−7653.
(24) Chen, J.-C.; Sun, Y.-S.; Tung, S.-H.; Chen, W.-C. *Soft Matter* **2012**, *8*, 526.
(25) Lohwasser, R. H.; Thelakkat, M. *Macromolecules* **2012**, *45*, 3070−3077.
(26) Gernigon, V.; Richard, F.; Leclerc, N.; Lévêque, P., Brochon, C.; Hadziioannou, G.; Heiser, T. Presented at the *European Material Research Society (E-MRS) Spring Conference, Symposium N*, Abstract No. 16−2, Nice, France, 2011.
(27) Jeffries-El, M.; Sauvé, G.; McCullough, R. D. *Macromolecules* **2005**, *38*, 10346.
(28) Richard, F. Thesis, University of Strasbourg: Strasbourg, France 2008.
(29) Garcia, R.; Pérez, R. *Surf. Sci. Rep.* **2002**, *47*, 197.
(30) Heiser, T.; Adamopoulos, G.; Brinkman, M.; Giovanella, U.; Ould-Saad, S.; Brochon, C.; Van de Wetering, K.; Hadziioannou, G. *Thin Solid Films* **2006**, *511−512*, 219−223.
(31) Sary, N.; Mezzenga, R.; Brochon, C.; Hadziioannou, G.; Ruokolainen, J. *Macromolecules* **2007**, *40*, 3277−3286.
(32) Treat, N. D.; Brady, M. A.; Smith, G.; Toney, M. F.; Kramer, E. J.; Hawker, C. J.; Chabinyc, M. L. *Adv. Energy Mater.* **2011**, *1*, 82.
(33) Carach, C.; Riisness, I.; Gordon, M. J. *Appl. Phys. Lett.* **2012**, *101*, 083302.
(34) Lee, Y. H.; Yen, W. C.; Su, W. F.; Dai, C. A. *Soft Matter* **2011**, *7*, 10429−10442.
(35) Spano, F. C. *J. Chem. Phys.* **2005**, *122*, 234701.
(36) Clark, J.; Silva, C.; Friend, R. H.; Spano, F. C. *Phys. Rev. Lett.* **2007**, *98*, 206406.
(37) Spano, F. C.; Clark, J.; Silva, C.; Friend, R. H. *J. Chem. Phys.* **2009**, *130*, 074904.
(38) Li, G.; Yao, Y.; Yang, H.; Shrotriya, V.; Yang, G.; Yang, Y. *Adv. Funct. Mater.* **2007**, *17*, 1636−1644.